J. Biochem. 2010;148(6):669–679 doi:10.1093/jb/mvq101

JB THE JOURNAL OF BIOCHEMISTRY

COOH-terminal isoleucine of lysosome-associated membrane protein-1 is optimal for its efficient targeting to dense secondary lysosomes

Received July 6, 2010; accepted August 25, 2010; published online September 2, 2010

Kenji Akasaki[1,*], Michihisa Suenobu[1], Maki Mukaida[1], Akihiro Michihara[1] and Ikuo Wada[2]

[1]Faculty of Pharmacy and Pharmaceutical Sciences, Fukuyama University, Fukuyama Hiroshima 729-0292; and [2]Department of Cell Science, Institute of Biomedical Sciences, Fukushima Medical University School of Medicine, Fukushima 960-1295, Japan

*Kenji Akasaki, Fukuyama University, Fukuyama Hiroshima 729-0292, Japan. Tel: +81 84 936 2111 (ext. 5235), Fax: +81 84 936 2024, email: akasaki@fupharm.fukuyama-u.ac.jp

Lysosome-associated membrane protein-1 (LAMP-1) consists of a highly glycosylated luminal domain, a single-transmembrane domain and a short cytoplasmic tail that possesses a lysosome-targeting signal (GYQTI^{382}) at the COOH terminus. It is hypothesized that the COOH-terminal isoleucine, I^{382}, could be substituted with any other bulky hydrophobic amino acid residue for LAMP-1 to exclusively localize in lysosomes. In order to test this hypothesis, we compared subcellular distribution of four substitution mutants with phenylalanine, leucine, methionine and valine at the COOH-terminus (termed I382F, I382L, I382M and I382V, respectively) with that of wild-type (WT)-LAMP-1. Double-labelled immunofluorescence analyses showed that these substitution mutants were localized as significantly to late endocytic organelles as WT-LAMP-1. However, the quantitative subcellular fractionation study revealed different distribution of WT-LAMP-1 and these four COOH-terminal mutants in late endosomes and dense secondary lysosomes. WT-LAMP-1 was accumulated three to six times more in the dense lysosomal fraction than the four mutants. The level of WT-LAMP-1 in late endosomal fraction was comparable to those of I382F, I382M and I382V. Conversely, I382L in the late endosomal fraction was approximately three times more abundant than WT-LAMP-1. These findings define the presence of isoleucine residue at the COOH-terminus of LAMP-1 as critical in governing its efficient delivery to secondary lysosomes and its ratio of lysosomes to late endosomes.

Keywords: COOH-terminal amino acid/glycoprotein/lysosome/membrane/targeting signal.

Abbreviations: AP, adaptor protein complex; EGFP, enhanced green fluorescent protein; LAMP, lysosome-associated membrane protein; NS, newly synthesized; PNS, post-nuclear supernatant; TGN, *trans*-Golgi network; WT, wild-type.

Lysosomes are cytoplasmic organelles involved in endocytic and auphagic processes and possess an assortment of soluble acid-dependent hydrolases and a set of integral membrane glycoproteins (*1–3*). Two structurally similar classes of lysosome-associated membrane proteins, LAMP-1 and LAMP-2, are major components of these membrane glycoproteins and occur in almost all cell types in birds and mammals (*4–8*). While LAMPs are localized predominantly in lysosomes, they are also found in endosomal compartments at a steady state (*9*). Furthermore, endogenous LAMP-1 and LAMP-2 shuttle between the cell surface and lysosomes through early and late endosomes (*10–13*). Both of the LAMPs consist of a large, extensively glycosylated luminal domain, a single transmembrane domain and a short cytoplasmic tail at the COOH-terminal. The cytoplasmic tails of LAMPs contain a consensus amino acid sequence (GYXXΦ) called a tyrosine-base motif for lysosomal targeting (*6–8*). Immunofluorescence studies using the site-directed mutants of LAMP-1 indicated that Φ could be any bulky hydrophobic amino acid for localization in late endosomes and lysosomes (*14–16*). In fact, F, I, M, L and V naturally occur in the Φ position of the lysosomal membrane proteins (*4–8*, *17–20*).

Newly synthesized (NS) lysosomal membrane proteins follow a common biosynthetic route from the endoplasmic reticulum to the *trans*-Golgi network (TGN). Two different pathways designated as 'direct' and 'indirect' have been proposed for biosynthetic transport from the TGN (*18*, *19*, *21–29*). In the direct pathway, they are transported intracellularly from the TGN to either early or late endosomes and then to lysosomes (*21*, *23–28*). In the indirect pathway, in contrast, NS lysosomal membrane proteins are transported from the TGN to the cell surface from which they are internalized and subsequently delivered to lysosomes *via* early and late endosomes (*19*, *22*, *29*). It has been shown that sorting events of LAMPs in the post-Golgi compartments (TGN, the cell surface and early endosomes) are mediated by four heterotetrameric adaptor protein complexes (i.e. AP-1, AP-2, AP-3 and AP-4) associated with coated vesicles involved in endocytic and late secretory pathways [reviewed in (*30–32*)]. Interaction of GYXXΦ motifs with one or two of these AP complexes is considered to help LAMPs incorporate into coated vesicles. Cytoplasmic peptides containing the tyrosine-based motif indeed bind to APs *in vitro* and the COOH-terminal amino acid (Φ) influences the ability

of the LAMPs cytoplasmic tails to interact with AP complexes (*33–37*). Three variants of avian LAMP-2 with different amino acid sequences in the transmembrane and cytoplasmic domains are differently distributed between the intracellular organelles and the cell surface (*17*, *18*). The different distribution is due to the difference of Φ of the targeting signal (*18*, *19*). Assuming from these results, the strength of interaction of APs with the tail could be related to the ratios of the cell surface to intracellular LAMP variants. The variants may interact selectively with APs associated with different sites of the sorting. Since the intracellular organelles represent mixtures of early endosomes, late endosomes and lysosomes, it is unclear whether difference of Φ exerts an effect(s) on distribution of LAMPs between endosomes and lysosomes. We have previously established separation conditions for these three endocytic organelles from cultured rat hepatocytes and human hepatoma cell lines using the Percoll density centrifugation method (*13*, *25*, *26*, *38*). This fractionation method combined with immunofluorescence microscopy enabled us to quantitatively analyse lysosomal membrane proteins partitioned in endosomes and lysosomes (*38*).

In the present study, we have undertaken comparative morphological and cell fractionation studies using cells that transiently express wild-type (WT)-LAMP-1 and its COOH-terminal amino acid substitution mutants to understand the role(s) of the COOH-terminal isoleucine in endosomal and lysosomal localization of LAMP-1. It is concluded from the results obtained here that the COOH-terminal isoleucine is optimal for efficient targeting of LAMP-1 to secondary lysosomes.

Materials and Methods

Materials

Anti-mouse LAMP-1 monoclonal antibody (1D4B) and a mammalian cell expression plasmid, pEGFP-Rab7, were kindly provided by Dr Thomas August (Johns Hopkins University, Baltimore, MD, USA) and Dr Marino Zerial (Max Planck Institute for Molecular Cell Biology and Genetics, Dresden, Germany), respectively. Antibodies used were as follows: anti-Rab5 polyclonal antibody (Santa Cruz Biotechnology, Inc.), anti-EEA1 mouse monoclonal antibody, anti-syntaxin 8 mouse monoclonal antibody and anti-human LAMP-1 mouse antibody (BD Biosciences). Anti-rat LAMP-1 and anti-green fluorescence protein (GFP) rabbit polyclonal antibodies were prepared in (*11*) and (*20*), respectively.

DNA constructs of site-directed mutants of LAMP-1

Mouse LAMP-1 cDNA, which had originally been cloned into M13 mp9 (*4*), was subcloned into the *Eco*RI site of pcDNA3.1 mammalian expression vector (Invirtogen, San Diego, CA, USA). COOH-terminal mutants were prepared using polymerase chain reaction (PCR) with the linear mouse LAMP-1 cDNA as a template using Prime Star Premix (Takara Suzo, Ohtzu, Japan). A forward primer is 5′-AGCAAAGAGATCTACACCATGGAT-3′ annealed to the sequence corresponding to amino acid residues S^{103} to D^{110}, 52 base pairs upstream of a unique *Eco*RV restriction site of mouse LAMP-1 cDNA (*4*, *15*). The following reverse primers were used to generate substitution mutants at I^{382} (primers are anti-sense, a codon corresponding to an exchanged amino acid is bold and an *Xba*I sites introduced into the primer is underlined):

I382A, 5′-GCCCATCTAGACTA**GGC**GGTCTGATAGCC-3′;
I382C, 5′-GCCCATCTAGACTA**ACA**GGTCTGATAGCC-3′;
I382D, 5′-GCCCATCTAGACTA**GTC**GGTCTGATAGCC-3′;
I382F, 5′-GCCCATCTAGACTA**GAA**GGTCTGATAGCC-3′;
I382M, 5′-GCCCATCTAGACTA**CAT**GGTCTGATAGCC-3′;
I382L, 5′-GCCCATCTAGACTA**CAA**GGTCTGATAGCC-3′;
I382V, 5′-GCCCATCTAGACTA**AAC**GGTCTGATAGCC-3′;
I382W, 5′-GCCCATCTAGACTA**CCA**GGTCTGATAGCC-3′.

The PCR products were purified using a PCR purification kit (Qiagen, Tokyo, Japan) and digested with *Eco*RV and *Xba*I. The pcDNA3.1 plasmid where the mouse LAMP-1 cDNA had been inserted at the *Eco*RI restriction site was cut with *Eco*RV and *Xba*I, and the insert resulting from this cut was removed. The enzyme-digested PCR product was ligated into the *Eco*RV and *Xba*I sites of the pcDNA3.1-mouse LAMP-1 cDNA. Competent *Escherichia coli* DH5α was transformed with pcDNA3.1 containing the mutant cDNA. The plasmid was purified from cultures of the transformed *E. coli* by the method of alkaline lysis using a plasmid purification kit (Qiagen). All mutants were confirmed by dideoxy sequencing.

Cell culture and transfection

COS7 cells were grown in Dulbecco's minimal essential medium (DMEM; Gibco ERL, Grand Island, NY, USA) supplemented with 10% foetal calf serum, 100 U/ml penicillin/streptomycin (Life Technologies Inc.) and 2 mM L-glutamine (Life Technologies Inc.). Confluent cells were passaged the day before transient transfection and 2×10^5 cells were distributed into a 35-mm plastic dish. Once cells reached 60% confluency, transient transfection of the above vectors was carried out with 5 μg of DNA using PolyFect (Qiagen) in 1 ml of DMEM according to the previous procedure (*20*). Transfected cells were then washed with phosphate buffered saline (PBS), overlaid with supplemented DMEM and left to incubate for 24 h. Normal rat kidney (NRK) cells were cultured under the same condition as COS7 cells.

Immunofluorescence microscopy

Cells were grown on glass coverslips and fixed with −20°C methanol for 4 min. Fixed cells were washed and blocked with 0.5% bovine serum albumin (BSA) in PBS. Cells were incubated sequentially in primary and secondary antibodies diluted in 0.5% BSA/PBS at room temperature for appropriate time and mounted with ProLong Antifade (Molecular Probe-Invitrogen, San Diego, CA, USA). Confocal images were collected using a laser-scanning microscope (Carl Zeiss model 510meta).

Cell fractionation

Confluent COS7 cells were washed two times with cold PBS, then with a cold isotonic sucrose solution 0.25 M sucrose/10 mM Tris–HCl (pH 7.2)/1 mM EDTA and then removed from the dish using a rubber policeman. The cells (3×10^6) in 1.5 ml of the isotonic sucrose solution containing a set of protease inhibitors (1 mM phenylmethylsulphonyl fluoride, 1 μg/ml leupeptin and 1 μg/ml pepstatin A) were disrupted and homogenized by nitrogen cavitation using Cell Disruption Bombs (Central Scientific Commerce Inc., Tokyo, Japan) under a pressure at 2400 kPa for 1 min and then centrifuged at 650*g* for 10 min. The post-nuclear supernatant (PNS) containing ∼1.0 mg of total proteins was diluted with Percoll to a final concentration of 30 (v/v)% and centrifuged at 25,000 rpm for 40 min in a Beckman 70.1 Ti rotor. Following centrifugation, the gradients were divided into 18×0.5 ml fractions by downward displacement. Solubilizing buffer was added to each fraction to a final concentration of 1% sodium dodecyl sulphate (SDS), 2 mM EDTA, 0.5% Lubrol PX, 0.15 M NaCl, 10 mM Tris–HCl (pH 7.0), 5 mM EDTA and protease inhibitor cocktail (Roche Applied Science, Tokyo, Japan). Percoll particles were precipitated by centrifugation for 1 h at 100,000*g* in a Beckman 70.1Ti rotor. An equal volume of the supernatants was analysed by quantitative immunoblotting as described below.

Sodium dodecyl sulfate-polyacrylamide gel electrophoresis and western immunoblot analysis

PNS and fractionated PNS were mixed with sample buffer, boiled for 3 min and loaded onto 12% acrylamide gel for sodium dodecyl sulfate-polyacrylamide gel electrophoresis (SDS–PAGE) according to the method of Laemmli (*39*). The separated proteins were electrotransferred to nitrocellurose sheets (Toyo Roshi Ltd, Tokyo, Japan) according to the method of Towbin *et al.* (*40*). The sheets were

blocked for 1 h in PBS containing 10% skim milk and 0.05% Tween-20 and incubated for 2 h at room temperature with an appropriate concentration of primary antibody in 0.05% Tween-20/0.2% skim milk/PBS. After five washes with 0.05% Tween-20/0.2% skim milk/PBS, the sheets were incubated for 2 h at room temperature with a 1/1,000 dilution of horseradish peroxidase-conjugated secondary antibody in 0.05% Tween-20/0.2% skim milk/PBS. Immuno reactive bands were detected using ECL detection kit (Amersham, Tokyo, Japan) according to the manufacturer's instructions. Densities of immunopositive bands were quantified with an Intelligent Quantifier (Bio Image, CA, USA) according to the method of Guengerich *et al.* (*41*).

Other procedures

Alkaline phosphodiestherase I and β-glucuronidase were assayed by Brightwell and Tappel (*42*) and Robins *et al.* (*43*), respectively.

Results

Expression of WT-LAMP-1 and its COOH-terminal substitution mutants

As depicted in Fig. 1A, we generated mammalian cell expression vectors containing cDNAs that encode mouse WT-LAMP-1 and different COOH-terminal mutants (I382D, I382F, I382M, I382L and I382V). COS7 cells were transfected with these plasmids and cultured for 24 h. PNSs of these cells were prepared as described under 'Materials and Methods' section. PNSs with similar protein concentrations and specific activities of β-glucuronidase were used for the cell fractionation. To examine the expression levels of exogenous WT-LAMP-1 and its mutants in the PNSs, they were simultaneously subjected to western immunoblot analysis. As shown in Fig. 1B, the WT-LAMP-1 and the mutant protein bands were stained in the transfected cells to similar extents, allowing us to perform comparative immunofluorescence and cell fractionation studies.

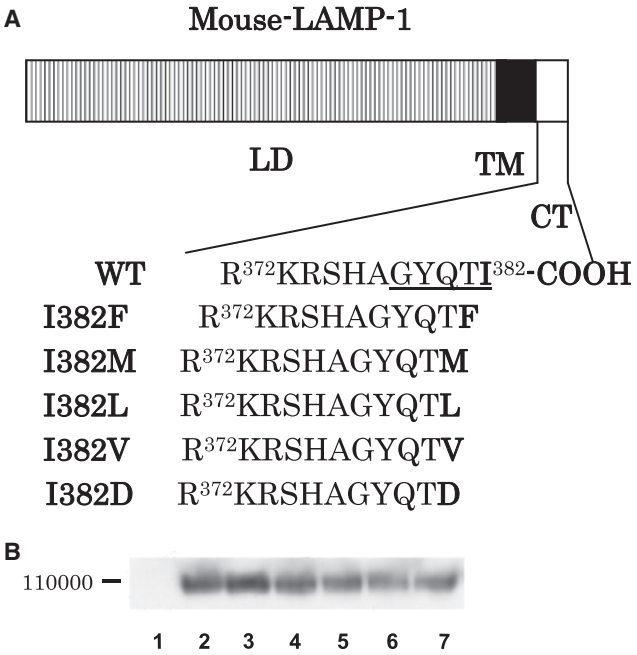

Fig. 1 Western immunoblot analysis of COS7 cells expressing WT-LAMP-1 and the COOH-terminal substitution mutants. (A) Schematic representation of WT-LAMP-1 and its substitution mutants at the COOH-terminus. Mouse WT-LAMP-1 is a 382-amino acid-polypeptide consisting of a large luminal domain (LD), a transmembrane domain (TM) and a short cytoplasmic tail (CT) at the COOH-terminus. The COOH-terminal five-amino acid sequence (GYQTI) for lysosomal targeting is underlined. The COOH-terminal isoleucine (I^{382}) was substituted with phenylalanine (I382F), methionine (I382M), leucine (I382L), valine (I382V) and aspartic acid (I382D) as described in 'Materials and Methods' section. (B) Equal amounts (~20 μg protein) of PNSs from COS7 cells transfected with the expression plasmids of WT-LAMP-1 and its mutants were simultaneously subjected to SDS–PAGE followed by western immunoblotting with anti-mouse LAMP-1 monoclonal antibody (1D4B). Lane 1, parental; lane 2, WT; lane 3, I382F; lane 4, I382V; lane 5, I382L; lane 6, I382M and lane 7, I382D. A molecular weight was indicated to the left.

Localization of WT-LAMP-1 and the COOH-terminal-mutants by confocal immunofluorescence microscopy

We analysed the cellular localization of WT-LAMP-1 and the COOH-terminal mutants in their respective cells by double-labelled immunofluorescence microscopy. Syntaxin 8, a class of SNARE proteins, was employed as an endogenous marker for late endocytic organelles (*44*). To ascertain whether endogenous syntaxin 8 resides in late endosomes and/or lysosomes, we compared its immunofluorescence patterns with those of endogenous LAMP-1 in NRK cells (Fig. 2A, *a–c*). Syntaxin 8 showed notable colocalization of LAMP-1 in the perinuclear region, attesting the significant localization of syntaxin 8 in late endocytic organelles. As shown in Fig. 2A *d–f*, WT-LAMP-1 was localized predominately to vesicles in perinuclear cytoplasm and markedly colocalized to syntaxin 8, similar to co-distribution of LAMP-1 and syntaxin 8 in NRK cells. Immunofluorescent signals of I382F (Fig. 2A, *p–r*), I382L (Fig. 2A, *s–u*), I382M (Fig. 2A, *g–i*) and I382V (Fig. 2A, *m–o*) were significantly detected in perinuclear vesicles containing syntaxin 8 in COS7 cells as observed for WT-LAMP-1. In an I382D-expressing cell (Fig. 2A, *j–l*), immunofluorescence with anti-LAMP-1 antibody labelled the plasma membrane and cytoplasmic vesicles devoid of syntaxin 8 signal. Additionally, I382D was concentrated close to a nucleus and some of I382D-positive perinuclear vesicles were labelled with anti-syntaxin 8 immunofluorescence. Syntaxin 8 is shown to reside in TGN-derived non-coated vesicles as well (*44*), suggesting that excess I382D is accumulated in the vesicles involved in secretory pathway.

Subcellular fractionation of COS7 cells

In the double-labelled immunofluorescence analyses, there were no notable differences in intracellular distribution among WT, I382F, I382M, I382L and I382V. To obtain further information on their intracellular localization, we next quantified these LAMP-1 variants distributed in the endocytic organelles, early endosomes, late endosomes and lysosomes, by the cell fractionation technique. We previously reported the separation of these three organelles from cultured rat hepatocytes and HepG2 cells with Percoll density centrifugation (*25*, *38*). In the present study, a similar isopycnic centrifugation procedure was applied for separation of the endocytic organelles of COS7 cells.

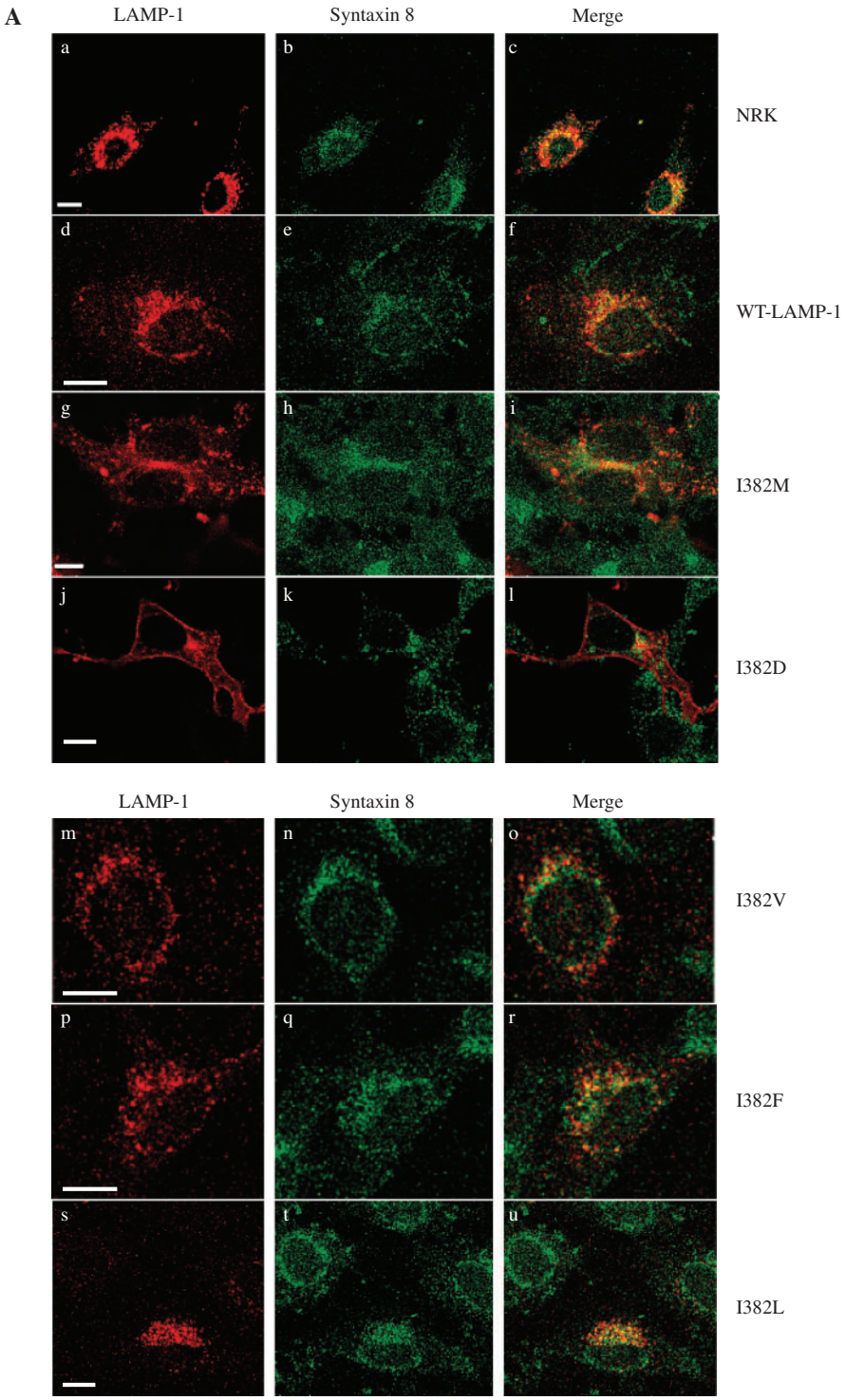

Fig. 2 Immunofluorescence localization of WT-LAMP-1 and its COOH-terminal mutants in their respective COS7 cells. (A) To determine the extent of endogenous LAMP-1 colocalized with endogenous syntaxin 8, NRK cells were analysed by double-immunofluorescence microscopy (*a*–*c*). The cells were fixed with methanol at −20°C, and stained with anti-rat LAMP-1 rabbit antibody followed by Alexa Fluor 594 (red)-coupled anti-rabbit IgG goat antibody (*a*) and anti-syntaxin 8 mouse antibody followed by Alexa Fluor 488 (green)-coupled anti-mouse IgG goat antibody (*b*). The images of *a* and *b* were merged into *c*. COS7 cells expressing WT-LAMP-1 (*d*–*f*), I382M (*g*–*i*), I382D (*j*–*l*), I382V (*m*–*o*), I382F (*p*–*r*) and I382L (*s*–*u*) were analysed by double-immunofluorescence microscopy. The cells were fixed with methanol at −20°C and stained with the following antibodies: anti-mouse LAMP-1 rat antibody followed by Alexa Fluor 594 (red)-coupled anti-rat IgG goat antibody (*d*, *g*, *j*, *m*, *p* and *s*) and anti-syntaxin 8 mouse antibody followed by Alexa Fluor 488 (green)-coupled anti-mouse IgG goat antibody (*e*, *h*, *k*, *n*, *q* and *t*). The images shown in *f*, *i*, *l*, *o*, *r* and *u* were obtained by overlaying red and green channels. (B) To examine colocalization of endogenous LAMP-1 and EEA1, NRK cells were analysed by double-immunofluorescence microscopy (*a*–*c*). The cells were fixed with methanol at −20°C, and stained with anti-rat LAMP-1 rabbit antibody followed by Alexa Fluor 594 (red)-coupled anti-rabbit IgG goat antibody (*a*) and anti-EEA1 mouse antibody followed by Alexa Fluor 488 (green)-coupled anti-mouse IgG goat antibody (*b*). The images of *a* and *b* were merged into *c*. COS7 cells transfected with cDNA encoding WT-LAMP-1 were fixed with methanol at −20°C and stained with the following antibodies: anti-mouse LAMP-1 rat antibody followed by Alexa Fluor 594 (red)-coupled anti-rat IgG goat antibody (*d*) and anti-EEA1 mouse antibody followed by Alexa Fluor 488 (green)-coupled anti-mouse IgG goat antibody. (*e*). The images of *d* and *e* were merged into *f*. Bars, 10 μm.

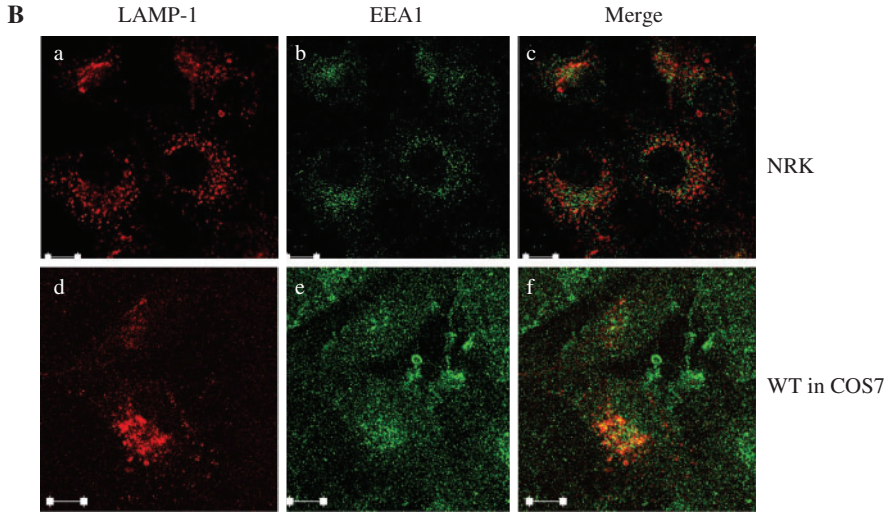

Fig. 2 Continued.

Alkaline phosphodiesterase I (APDE I) and β-glucuronidase activities were measured to locate fractions containing the plasma membrane and lysosomes in the Percoll gradient, respectively. As shown in Fig. 3A, APDE I displayed a single peak at fraction 3 of light buoyant density. Two peaks of β-glucuronidase were observed in fractions 5 and 17. A major peak of β-glucuronidase in the densest fraction is originated from typical dense lysosomes (secondary lysosomes) whereas the enzymic activities detected in the light buoyant density fraction are from microsomal β-glucuronidase as described previously (*25*, *26*). We further determined the distribution of Rab5, a marker for early endosomes (*45*), on the Percoll gradient (Fig. 3B). Rab5 is localized in the low buoyant density fraction with a single peak (fraction 4) between the plasma membrane and the endoplasmic reticulum. Location of late endosomes was subsequently examined by means of transgened EGFP-Rab7 because of exclusive localization of Rab7 in late endosomes (*45*). As shown in Fig. 3C, EGFP-Rab7 was distributed mainly between fractions 10 and 14 with an intermediate buoyant density. Distributions of these endocytic organelles of COS7 cells in Percoll density gradient are similar to those of hepatic cells (*25*, *38*). Taken together with these results, the isopycnic centrifugation allowed us to well separate early endosomes, late endosomes and lysosomes.

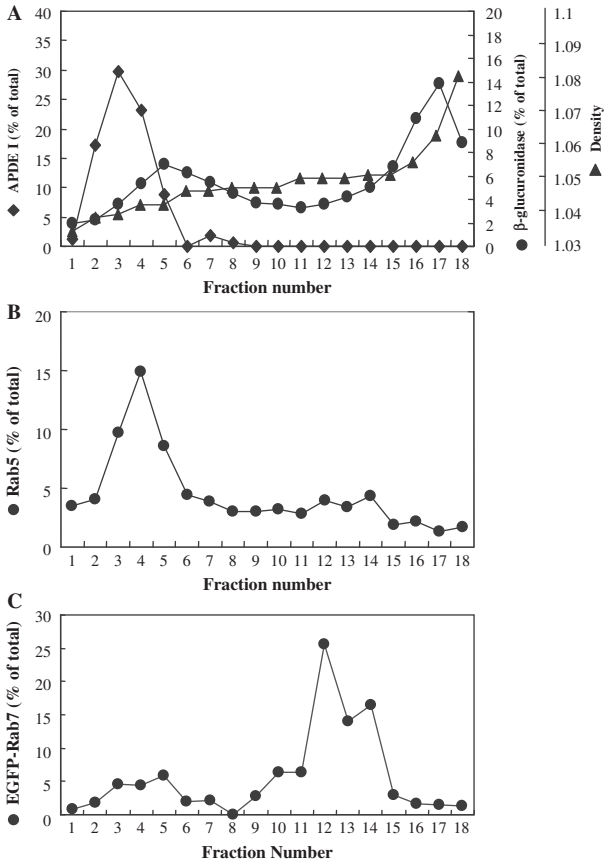

Fig. 3 Distribution of marker proteins for endocytic organelles in the Perocoll gradient. (A) PNS of COS7 cells was fractionated by the Percoll density gradient centrifugation. Fractions of 0.5 ml were collected from the top of the gradient. Activities of alkaline phosphodiesterase I (APDE I; closed squares) and β-glucuronidase (closed circles) were assayed. (B) For distribution of Rab5, equivalent volumes of the fractions were subjected to SDS–PAGE followed by western immunoblotting using anti-Rab5 antibody. Densities of positive bands were the quantified by densitometric tracing. An amount of Rab5 in each fraction was expressed as percentage of the total. (C) For distribution of Rab7, PNS of COS7 transfected with *pEGFP-Rab7* was fractionated with the Percoll density centrifugation. The fractions were subjected to western immunoblotting with anti-GFP antibody. The densities of positive bands were analysed by densitometry and an amount of Rab7-EGFP in each fraction was expressed as percentage of the total.

WT-LAMP-1 and the COOH-terminal mutants are differently distributed in the Percoll gradient

We investigated the distribution of WT-LAMP-1 and the five COOH-terminal mutants in the Percoll density gradient using quantitative western immunoblotting. Figures 4 and 5 showed the distribution patterns of exogenous WT-LAMP-1 and the mutants, respectively. Figure 6 indicated their relative abundances in late endosomes and lysosomes. As shown in Fig. 4A, ~70% of the total WT-LAMP-1 was recovered in the light equilibrium density fraction containing the plasma membrane and early endosomes, whereas

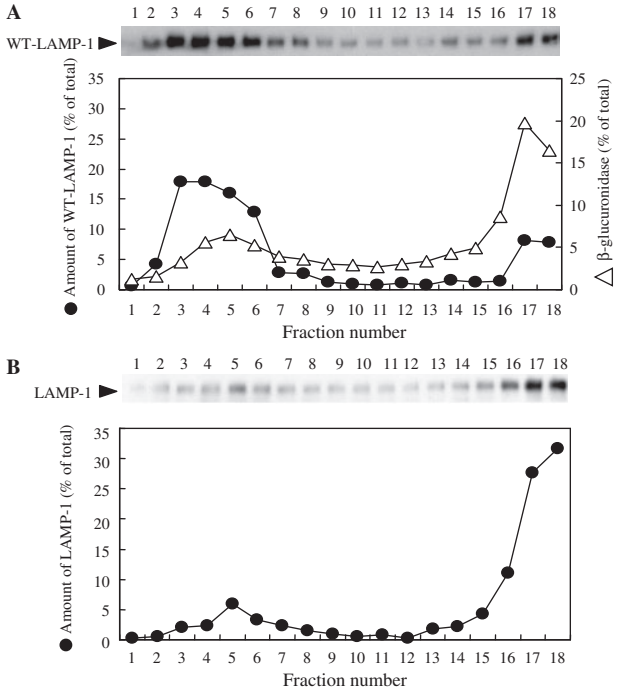

Fig. 4 Distribution of exogenous and endogenous WT-LAMP-1 in the Percoll gradient fractions. PNS of COS7 cells expressing WT-LAMP-1 was fractionated by the Percoll density gradient centrifugation. Equivalent volumes of the fraction were subjected to western immunoblotting with anti-mouse and anti-human LAMP-1 antibodies for exogenous (A) and endogenous (B) LAMP-1 molecules, respectively, and to β-glucuronidase assay. The resultant blots with fraction numbers were shown in the upper panels. The lower panels showed the quantification of the blots (closed circles) and β-glucuronidase (open triangles). The amounts of exogenous (A) and endogenous (B) WT-LAMP-1, and β-glucuronidase (A) in the Percoll density fractions were expressed as percentage of the total. Similar findings were obtained in at least three independent experiments.

∼15% of the total was present in the densest lysosomal fraction. WT-LAMP-1 was broadened through fractions 10 to 14, giving a small yield of ∼2%. In contrast, a major portion of endogenous simian LAMP-1 was located in the densest lysosomal fraction (Fig. 4B). The distribution pattern of endogenous LAMP-1 was very similar to that of β-glucuronidase (Fig. 4A) and almost the same as that of endogenous LAMP-1 in parental COS7 cells without transfection (data not shown). Therefore, it is likely that the expression of exogenous WT-LAMP-1 does not affect the intracellular distribution of endogenous LAMP-1. In COS7 cells generating I382F (Fig. 5A), I382M (Fig. 5B), I382L (Fig. 5C) and I382V (Fig. 5D), large portions of these mutants were deposited in the light buoyant density fraction and smaller portions of them were present in the densest lysosomal fraction. The quantitative analyses revealed that lysosomal I382F, I382M, I382L and I382V account for 3–5% of the total (Fig. 6B). The levels of these mutants in the dense lysosomal fraction were 3–5 times lower than that of WT-LAMP-1 (Fig. 6B). It was characteristic that I382L was notably broadened through the intermediate fraction (fractions 10 to 14) containing late endosomes (Fig. 5C), resulting in the highest abundance of I382L in the late endosomal fraction among WT- and the mutant LAMP-1 proteins (Fig. 6A). In the previous study by Gough *et al.* (*19*), the LAMP chimera with GYQSI and GYQSL as lysosomal targeting signals had the highest intracellular percentage among the other COOH-terminal substitution mutants, which agrees with the data presented here. As shown in Fig. 5E, I382D provided a single peak at the plasma membrane fraction but no positive signal in the intermediate and dense fraction, which was concomitant with the immunofluorescence microscopic observation (Fig. 2A, *j–l*). Additionally, the distribution profiles of I382A, I382C and I382W were analogous to that of I382D (data not shown). Since β-glucuronidase distribution in these transfected cells are very similar to each other (Fig. 4A and Fig. 5A–E), the differences of WT-LAMP-1 and its mutants in the Percoll density gradient distribution are not due to changes of lysosomal densities in the cells that overly express the LAMP-1 proteins.

When the distribution pattern of WT-LAMP-1 was compared with that of I382D, a notable portion of WT-LAMP-1 broadened to slightly denser fractions containing early endosomes (compared Fig. 4A with Fig. 5E), suggesting that a large amount of WT-LAMP-1 was accumulated in early endosomes. To verify whether excess WT-LAMP-1 is retained in early endosomes, its colocalization with early endosome-associated antigen 1(EEA1) (*46*) in COS7 cells was examined by the double-labelled immunofluorescence analysis. As shown in Fig 2B, *d–f*, WT-LAMP-1 was costained partially but substantially with EEA1 in COS7 cells that expressed WT-LAMP-1. On the other hand, endogenous LAMP-1 was hardly colocalized with EEA1 in NRK cells (Fig. 2B, *a–c*), which was consistent with the present (Fig. 4B) and the previous results (*25*, *26*) that low levels of endogenous LAMP-1 and LAMP-2 were present in early endosomes at a steady state. Furthermore, small amounts of WT-LAMP-1 were recovered in the plasma membrane and early endosomal fractions with the light buoyant density in Percoll density gradient from a stable HepG2 cell line that displays its moderate expression (Akasaki *et al.* unpublished data) as observed for endogenous LAMP-1 in COS7 cells (Fig. 4B). Harter and Mellman (*24*) have shown that increased biosynthesis of LAMP-1 caused its elevation on the plasma membrane. Therefore, the present quantitative fractionation study revealed that overexpression of exogenous WT-LAMP-1 resulted in its accumulation as much in the plasma membrane fraction as in the early endosomal fraction.

Optimal size and hydrophobicity of the COOH-terminal amino acid side chain is important for efficient trafficking of LAMP-1 to secondary lysosomes

To clarify whether the extents of hydrophobicity and side chain size of the COOH-terminal amino acid correlate with efficiency of lysosomal targeting, the levels in the lysosomal fraction were plotted against the Kite and Doolittle hydrophathy index (*47*) and against accessible surface area of the COOH-terminal

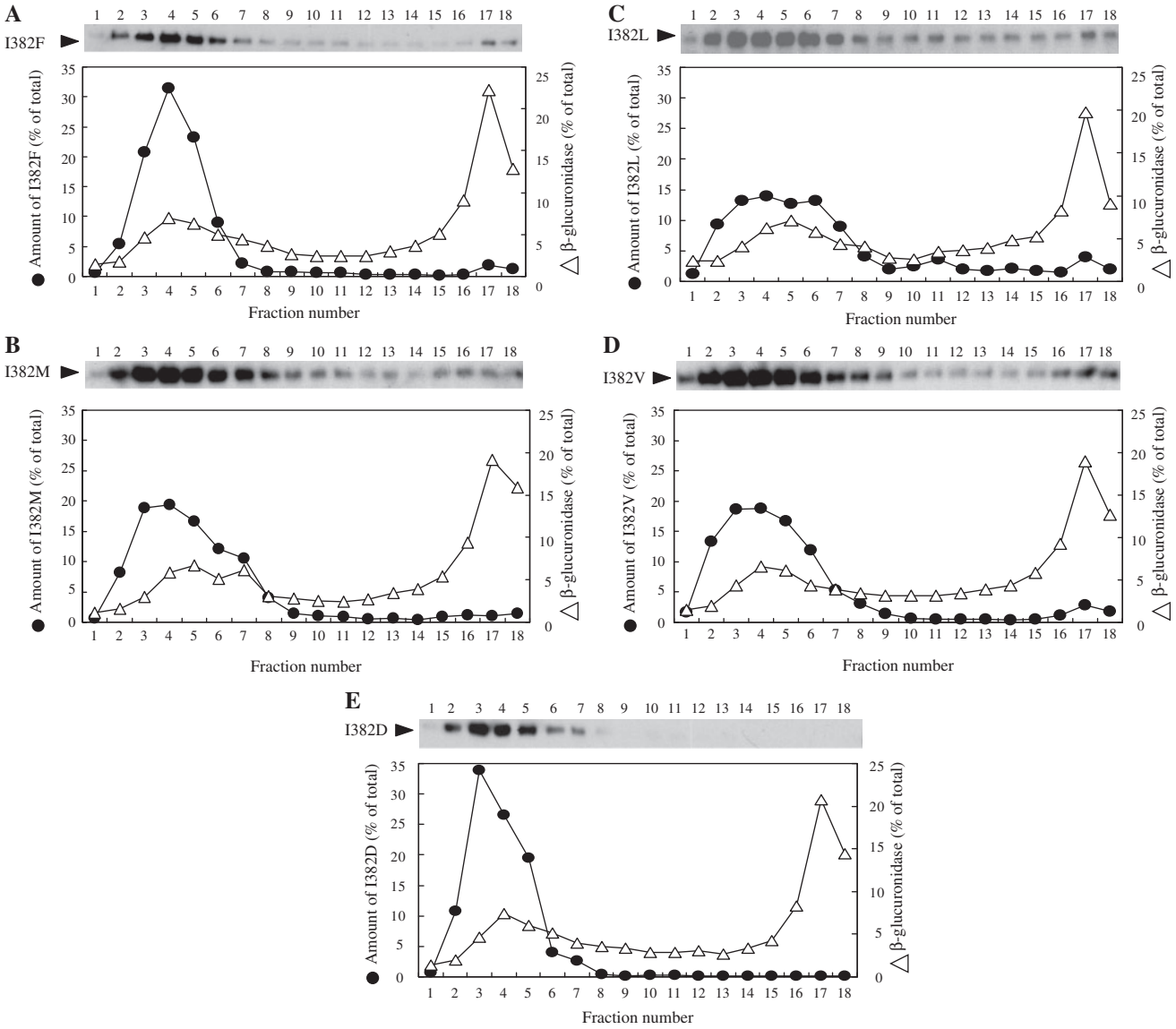

Fig. 5 The COOH-terminal point-mutated LAMP-1 (I382F, I382M, I382L, I382V, I382D) in the Percoll gradient fractions. PNSs of COS7 cells expressing I382F (A), I382M (B), I382L (C), I382V (D) and I382D (E) were fractionated by Percoll density gradient centrifugation. Equivalent volumes of the fraction were subjected to western immunoblotting with anti-mouse LAMP-1 antibody and to β-glucuronidase assay. The lower panels show the quantification of the blots (closed circles) and β-glucuronidase (open triangles). The amounts of the mutants and β-glucuronidase in the Percoll density fractions were expressed as percentage of the total. Similar findings were obtained in at least three independent experiments.

side chain (*48*), respectively. As shown in Fig. 7A, it is likely that LAMP-1 proteins ending in more hydrophobic amino acid residues have a tendency for more lysosomal localization. When the accessible surface area of COOH-terminal amino acid was plotted against the percentage of lysosomal WT-LAMP-1 and its mutants (Fig. 7B), a sharp peak was obtained at 180 $Å^2$, indicating that the COOH-terminal amino acid of LAMP-1 has an optimal size of the hydrophobic side chain for efficient lysosomal targeting.

Discussion

Two types of the targeting signals have thus far been identified in the COOH-terminal cytoplasmic tails of several classes of lysosomal membrane glycoproteins (*6–8*). One is a tyrosine-based motif representing GYXXΦ and the other is a di-leucine motif. The GYXXΦ sequence is found in LAMP-1 (*4*), LAMP-2 (*5*, *17*), DC-LAMP (*20*), CD63 (LIMP-1, LAMP-3) (*36*) and Endolyn (*37*) (has exceptionally an NYXXΦ). Isoleucine, leucine, methionine, phenylalanine and valine occur naturally at the COOH-terminus of these lysosomal membrane proteins. LAMP-1 mutants with these amino acid residues at the COOH terminus were all colocalized with endogenous syntaxin 8 in late endocytic organelles when analysed by double-labelled immunofluorescence microscopy. Gough *et al.* (*19*) conducted similar experiments with cells expressing LAMP-2 chimeras that have sequences of GYQSF, GYQSI, GYQSL, GYQSM and GYQSV and have shown that these LAMP chimeras coexist

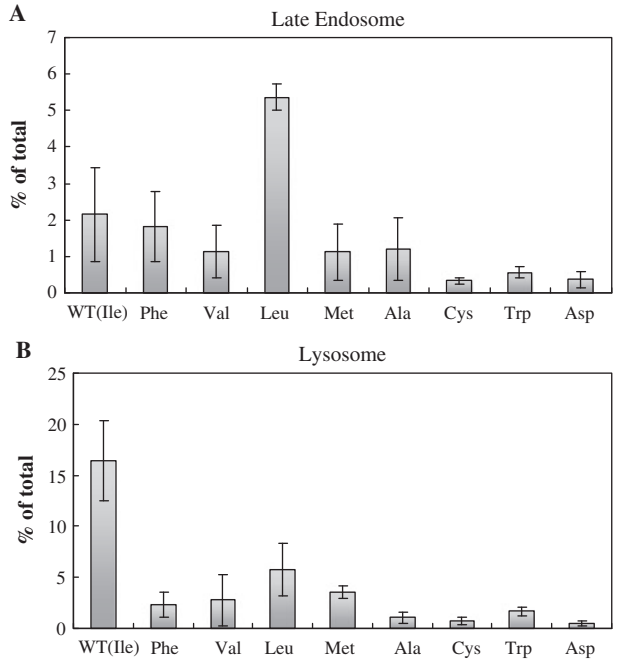

Fig. 6 Relative abundances of WT-LAMP-1 and the COOH-terminal mutants in late endosomal and lysosomal fractions. Relative abundances (percentage of the total) of WT-LAMP-1 and the mutants in late endosomes (A) and lysosomes (B) were measured by the Percoll density fractionation as described in the legend of Fig. 4. Late endosomal and lysosomal WT-LAMP-1 and the mutants are sums of those in fractions 10–14 and fractions 15–18, respectively. The data represent the average and standard deviation of at least three independent experiments.

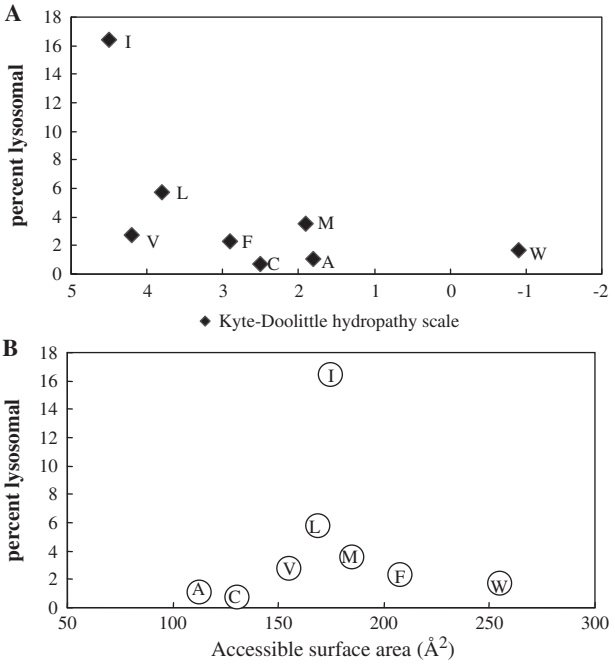

Fig. 7 Efficiency of lysosomal targeting against hydrophobicity and side chain size of the COOH-terminal amino acid. Lysosome targeting is indicated as the percent WT-LAMP-1 and the mutants in dense lysosomal fraction determined by the Percoll density gradient fractionation as shown in Figs 4 and 5. The hydrophobicity (A) and side chain size (B) are based on Kyte–Doolittle scale and accessible surface area of the COOH-terminal amino acid residue, respectively.

with endogenous LAMP-1 by double-labelled immunofluorescence microscopy, concomitant with our morphological observation. It is well known that LAMP-1 and LAMP-2 are distributed mainly in late endosomes and lysosomes, and to a lesser extent in early endosomes (*2*, *3*, *9*, *25*, *26*). Double-immunofluorescence microscopic analyses hardly discriminate between late endosomal and lysosomal LAMPs. In the present study, we successfully separated early endosomes, late endosomes and lysosomes by cell fractionation with the Percoll density gradient centrifugation as previously studied (*25*, *38*). Although the major portion of overexpressed WT-LAMP-1 and its COOH-terminal mutants resided in the plasma membrane and early endosomal fractions, we were able to measure precisely their localization in late endosomes and lysosomes. As an important result, WT-LAMP-1 with isoleucine at the COOH-terminus represented the highest percentage in the lysosomal fraction. Gough *et al.* (*18*, *19*) determined the ratio of the LAMP chimeras with various COOH-terminal amino acid residues at the cell surface to the total by the cell surface-binding assay with a specific antibody and have shown that their cell surface levels vary depending on the COOH-terminal amino acid residues. Since the cell surface-binding assay provided a percentage of intracellular LAMP proteins consisting of those in early endosomal, late endosomal and lysosomal fractions, our experimental results show for the first time the exact relationship between net lysosomal contents of LAMP-1 and nature of the COOH-terminal amino acid. It is therefore noteworthy that a single peak was obtained at the size of isoleucine residue when the lysosomal abundance was plotted against accessible surface area of the COOH-amino acid residue (Fig. 7B). Together with the fact that no other variant of the signal of LAMP-1 signal other than that of GYQTI occurs among all species identified (*4*, *6–8*), this isoleucine-terminated sequence is critical for the most efficient transport of LAMP-1 to secondary lysosomes. While the COOH-terminal leucine residue provides the second highest lysosomal targeting efficiency, it gives the highest level in late endosomal fraction. Another type of lysosomal membrane glycoprotein termed LGP85 or LIMP-2 has an LI signal of the di-leucine motif in the COOH-terminal cytoplasmic tail for lysosomal targeting (*6–8*). We have previously shown that site-directed mutagenesis at the COOH-terminal side isoleucine residue of the motif in LGP85 alters its distribution between late endosomes and lysosomes (*38*) and ~25% and 45% of WT-LGP85 were located in late endosomes and lysosomes, respectively. In contrast, LGP85 mutant with the LL sequence displays an adverse distribution with 35 and 13% in late endosomes and lysosomal fractions, respectively. As observed for LGP85, the replacement of COOH-terminal isoleucine with leucine changed the ratios of late endosomal/lysosomal LAMP-1 even though isoleucine and leucine have almost the same size of bulky side chain and very similar hydrophobicities.

Therefore, strict sorting machineries recognize identity of the COOH-terminal isoleucine and confer an equilibrium of LAMP-1 with its content being several times higher in lysosomes than in late endosomes.

There have been a body of evidence concerning machineries by which lysosomal membrane proteins are sorted to lysosomes [reviewed by Luzio *et al*. (*3*)]. The best characterized protein molecules that interact with cytoplasmic tails of LAMPs are APs associated with transport vesicles with and/or without clathrin (*30*–*32*). AP-1, AP-2 and AP-3 have been shown to bind to the lysosomal targeting sequence of cytoplasmic peptides of LAMP-1 and LAMP-2 *in vitro* (*33*–*37*). AP-3 but not AP-1 deficiency caused an increased trafficking of LAMPs to the cell surface (*36*, *37*, *49*–*51*). Although evidence was seemingly accumulated to suggest that AP-3 plays an important role in sorting LAMPs to lysosomes in TGN and early endosome-derived tubular network, the recent study has shown a significant function of AP-2 in the biosynthetic transport of LAMP-1 and LAMP-2 to late endosomes and then to lysosomes (*29*). As shown in Fig. 4A, LAMP-1 accumulated as much in early endosomal fractions as in the plasma membrane, suggesting that whether NS-LAMP-1 takes any of the direct and indirect routes, its passage through early endosomes containing AP-3 is a regulatory step for LAMPs transport to lysosomes. Ohno *et al*. (*34*) provided biochemical evidence that μ3A chain of AP-3 prefers I and L but disfavours F, M and V at the COOH-terminus of GYXXΦ sequence. Gough *et al*. (*19*) have later examined interactions of GYQSV of LAMP-2b and its COOH- terminal substitution peptides with μ3A chain. GYQSL, GYQSI and GYQSF displayed high affinities with μ3A chain whereas GYQSM and GYQSV had a lower and no affinity, respectively. Assuming that GYXXΦ signals ending in I and L interact more strongly with μ3A than the signals ending in F, M and V according to μ3As preferences, higher levels of WT-LAMP-1 ending in I and I382L (identical to the signal sequence of LAMP-2c) in late endosomes and lysosomes could be correlated to higher affinities with AP-3, supporting importance of AP-3 involved in a sorting machinery at the early endosomal stage in determining an amount of LAMP-1 delivered to late endosomes/lysosomes.

Together with observations elsewhere (*9*, *52*–*55*), our previous studies (*25*, *26*) indicate bi-directional flow of lysosomal membrane proteins between late endosomes and lysosomes. There have been several models for the mechanism of trafficking from late endosomes to lysosomes [reviewed in (*3*)]. A fusion model currently appears preferential in the relationship between these two endocytic organelles (*54*, *55*). Late endosomes fuse with lysosomes, resulting in formation of hybrid organelles in which endocytic materials are degraded. Thereafter, lysosomes re-form from the hybrid organelles with retrieval and/or recycling of some membrane proteins. According to this model, after NS-LAMP-1 is included into the hybrid organelles from late endosomes, a significant fraction of NS-LAMP-1 together with pre-existing LAMP-1 is transferred to re-forming lysosomes. I^{382} would determine a ratio of antegrade to retrograde LAMP-1 trafficking at the retrieval step.

Traub *et al*. (*56*) have shown that clathrin-coated vesicles containing AP-2 assemble on dense lysosomes. The vesicles with AP-2 appear to mediate retrograde transport out of lysosomes. AP-2 reportedly favours GYXXL but disfavours GYXXI. In fact, GYQTI does not bind to μ2-chain *in vitro* (*34*). Hence, I382L but not WT is possibly included into the AP-2-containing vesicles for backward traffic from lysosomes, leaving a higher amount of WT in lysosomes than that of I382L.

Funding
This work was supported by the Research Fund of Fukuyama University.

Conflict of interest
None declared.

References

1. Holtzman, E. (1989) *Lysosomes*, Plenum Press, New York
2. Kornfeld, S. and Mellman, I. (1989) The biogenesis of lysosomes. *Annu. Rev. Cell Biol.* **5**, 483–525
3. Luzio, J.P., Pryor, P.R., and Bright, N.A. (2007) Lysosomes: fusion and function. *Nat. Rev. Mol. Cell Biol.* **8**, 622–632
4. Chen, J.W., Cha, Y., Yuksel, K.U., Gracy, R.W., and August, J.T. (1988) Isolation and sequencing of a cDNA clone encoding lysosomal membrane glycoprotein mouse LAMP-1. Sequence similarity to proteins bearing onco-differentiation antigens. *J. Biol. Chem.* **263**, 8754–8758
5. Cha, Y., Holland, S.M., and August, J.T. (1990) The cDNA sequence of mouse LAMP-2. Evidence for two classes of lysosomal membrane glycoproteins. *J. Biol. Chem.* **265**, 5008–5013
6. Fukuda, M. (1991) Lysosomal membrane glycoproteins. Structure, biosynthesis, and intracellular trafficking. *J. Biol. Chem.* **266**, 21327–21330
7. Hunziker, W. and Geuze, H.J. (1996) Intracellular trafficking of lysosomal membrane proteins. *Bioessays* **18**, 379–389
8. Eskelinen, E.L., Tanaka, Y., and Saftig, P. (2003) At the acidic edge: emerging functions for lysosomal membrane proteins. *Trends Cell Biol.* **13**, 137–145
9. Griffiths, G., Hoflack, B., Simons, K., Mellman, I., and Kornfeld, S. (1988) The mannose 6-phosphate receptor and the biogenesis of lysosomes. *Cell* **52**, 329–341
10. Lippincott-Schwartz, J. and Fambrough, D.M. (1987) Cycling of the integral membrane glycoprotein, LEP100, between plasma membrane and lysosomes: kinetic and morphological analysis. *Cell* **49**, 669–677
11. Furuno, K., Ishikawa, T., Akasaki, K., Yano, S., Tanaka, Y., Yamaguchi, Y., Tsuji, H., Himeno, M., and Kato, K. (1989) Morphological localization of a major lysosomal membrane glycoprotein in the endocytic membrane system. *J. Biochem.* **106**, 708–716
12. Furuno, K., Yano, S., Akasaki, K., Tanaka, Y., Yamaguchi, Y., Tsuji, H., Himeno, M., and Kato, K. (1989) Biochemical analysis of the movement of a major lysosomal membrane glycoprotein in the endocytic membrane system. *J. Biochem.* **106**, 717–722

13. Akasaki, K., Fukuzawa, M., Kinoshita, H., Furuno, K., and Tsuji, H. (1993) Cycling of two endogenous lysosomal membrane proteins, lamp-2 and acid phosphatase, between the cell surface and lysosomes in cultured rat hepatocytes. *J. Biochem.* **114**, 598–604
14. Williams, M.A. and Fukuda, M. (1990) Accumulation of membrane glycoproteins in lysosomes requires a tyrosine residue at a particular position in the cytoplasmic tail. *J. Cell Biol.* **111**, 955–966
15. Guarnieri, F.G., Arterburn, L.M., Penno, M.B., Cha, Y., and August, J.T. (1993) The motif Tyr-X-X-hydrophobic residue mediates lysosomal membrane targeting of lysosome-associated membrane protein 1. *J. Biol. Chem.* **268**, 1941–1946
16. Höning, S. and Hunziker, W. (1995) Cytoplasmic determinants involved in direct lysosomal sorting, endocytosis, and basolateral targeting of rat lgp120 (lamp-I) in MDCK cells. *J. Cell Biol.* **128**, 321–332
17. Hatem, C.L., Gough, N.R., and Fambrough, D.M. (1995) Multiple mRNAs encode the avian lysosomal membrane protein LAMP-2, resulting in alternative transmembrane and cytoplasmic domains. *J. Cell Sci.* **108**, 2093–2100
18. Gough, N.R. and Fambrough, D.M. (1997) Different steady state subcellular distributions of the three splice variants of lysosome-associated membrane protein LAMP-2 are determined largely by the COOH-terminal amino acid residue. *J. Cell Biol.* **137**, 1161–1169
19. Gough, N.R, Zweifel, M.E., Martinez-Augustin, O., Aguilar, R.C., Bonifacino, J.S., and Fambrough, D.M. (1999) Utilization of the indirect lysosome targeting pathway by lysosome-associated membrane proteins (LAMPs) is influenced largely by the C-terminal residue of their GYXXΦ targeting signals. *J. Cell Sci.* **112**, 4257–4269
20. Akasaki, K., Nakamura, N., Tsukui, N., Yokota, S., Murata, S., Katoh, R., Michihara, A., Tsuji, H., Marques Jr, E.T.A., and August, J.T. (2004) Human dendritic cell lysosome-associated membrane protein expressed in lung type II pneumocytes. *Arch. Biochem. Biophys.* **425**, 147–157
21. Green, S.A., Zimmer, K.P., Griffiths, G., and Mellman, I. (1987) Kinetics of intracellular transport and sorting of lysosomal membrane and plasma membrane proteins. *J. Cell Biol.* **105**, 1227–1240
22. Nabi, I.R., Le Bivic, A., Fambrough, D., and Rodriguez-Boulan, E. (1991) An endogenous MDCK lysosomal membrane glycoprotein is targeted basolaterally before delivery to lysosomes. *J. Cell Biol.* **115**, 1573–1584
23. Carlsson, S.R. and Fukuda, M. (1992) The lysosomal membrane glycoprotein lamp-1 is transported to lysosomes by two alternative pathways. *Arch. Biochem. Biophys.* **296**, 630–639
24. Harter, C. and Mellman, I. (1992) Transport of the lysosomal membrane glycoprotein lgp120 (lgp-A) to lysosomes does not require appearance on the plasma membrane. *J. Cell Biol.* **117**, 311–325
25. Akasaki, K., Michihara, A., Mibuka, K., Fujiwara, Y., and Tsuji, H. (1995) Biosynthetic transport of a major lysosomal membrane glycoprotein, lamp-1: convergence of biosynthetic and endocytic pathways occurs at three distinctive points. *Exp. Cell Res.* **220**, 464–473
26. Akasaki, K., Michihara, A., Fujiwara, Y., Mibuka, K., and Tsuji, H. (1996) Biosynthetic transport of a major lysosome-associated membrane glycoprotein 2, lamp-2: a significant fraction of newly synthesized lamp-2 is delivered to lysosomes by way of early endosomes. *J. Biochem.* **120**, 1088–1094
27. Cook, N.R., Row, P.E., and Davidson, H.W. (2004) Lysosome associated membrane protein 1 (Lamp1) traffics directly from the TGN to early endosomes. *Traffic* **5**, 685–699
28. Niwa, K., Tanaka, R., Murase, H., Ishikawa, T., Fujita, H., Himeno, M., and Tanaka, Y. (2003) Two lysosomal membrane proteins, LGP85 and LGP107, are delivered to late endosomes/lysosomes through different intracellular routes after exiting from the *trans*-Golgi network. *Biochem. Biophys. Res. Commun.* **301**, 833–840
29. Janvier, K. and Bonifacino, J.S. (2005) Role of the endocytic machinery in the sorting of lysosome-associated membrane proteins. *Mol. Biol. Cell* **16**, 4231–4242
30. Bonifacino, J.S. and Dell'Angelica, E.C. (1999) Molecular bases for the recognition of tyrosine-based sorting signals. *J. Cell Biol.* **145**, 923–926
31. Owen, D.J., Collins, B.M., and Evans, P.R. (2004) Adaptors for clathrin coats: structure and function. *Annu. Rev. Cell Dev. Biol.* **20**, 153–191
32. Robinson, M.S. (2004) Adaptable adaptors for coated vesicles. *Trends Cell Biol.* **14**, 167–174
33. Höning, S., Griffith, J., Geuze, H.J., and Hunziker, W. (1996) The tyrosine-based lysosomal targeting signal in lamp-1 mediates sorting into Golgi-derived clathrin-coated vesicles. *EMBO J.* **15**, 5230–5239
34. Ohno, H., Aguilar, R.C., Yeh, D., Taura, D., Saito, T., and Bonifacino, J.S. (1998) The medium subunits of adaptor complexes recognize distinct but overlapping sets of tyrosine-based sorting signals. *J. Biol. Chem.* **273**, 25915–25921
35. Stephens, D.J. and Banting, G. (1998) Specificity of interaction between adaptor-complex medium chains and the tyrosine-based sorting motifs of TGN38 and lgp120. *Biochem. J.* **335**, 567–572
36. Rous, B.A., Reaves, B.J., Ihrke, G., Briggs, J.A.G., Gray, S.R., Stephens, D.J., Banting, G., and Luzio, J.P. (2002) Role of adaptor complex AP-3 in targeting wild-type and mutated CD63 to lysosomes. *Mol. Biol. Cell* **13**, 1071–1082
37. Ihrke, G., Kyttälä, A., Russell, M.R.G., Rous, B.A., and Luzio, J.P. (2004) Differential use of two AP-3-mediated pathways by lysosomal membrane proteins. *Traffic* **5**, 946–962
38. Tabuchi, N., Akasaki, K., and Tsuji, H. (2002) Ile(476), a constituent of di-leucine-based motif of a major lysosomal membrane protein, LGP85/LIMP II, is important for its proper distribution in late endosomes and lysosomes. *Biochem. Biophys. Res. Commun.* **295**, 149–156
39. Laemmli, U.K. (1970) Cleavage of structural proteins during the assembly of the head of bacteriophage T4. *Nature* **227**, 680–685
40. Towbin, H., Staehelin, T., and Gordon, J. (1979) Electrophoretic transfer of proteins from polyacrylamide gels to nitrocellulose sheets: procedure and some applications. *Proc. Natl Acad. Sci. USA* **76**, 4350–4354
41. Guengerich, F.P., Wang, P., and Davidson, N.K. (1982) Estimation of isozymes of microsomal cytochrome P-450

in rats, rabbits, and humans using immunochemical staining coupled with sodium dodecyl sulfate-polyacrylamide gel electrophoresis. *Biochemistry* **21**, 1698–1706
42. Brightwell, R. and Tappel, A.L. (1968) Subcellular distributions and properties of rat liver phosphodiesterases. *Arch. Biochem. Biophys.* **124**, 325–332
43. Robins, E., Hirsch, H.E., and Emmons, S.S. (1968) Glycosidases in the nervous system. I. Assay, some properties, and distribution of β-galactosidase, β-glucuronidase, and β-glucosidase. *J. Biol. Chem.* **243**, 4246–4252
44. Prekeris, R., Yang, B., Oorschot, V., Klumperman, J., and Scheller, R.H. (1999) Differential roles of syntaxin 7 and syntaxin 8 in endosomal trafficking. *Mol. Biol. Cell* **10**, 3891–3908
45. Chavrier, P., Parton, R.G., Hauri, H.P., Simons, K., and Zerial, M. (1990) Localization of low molecular weight GTP binding proteins to exocytic and endocytic compartments. *Cell* **62**, 317–329
46. Simonsen, A., Lippe, R., Christoforidis, S., Gaullier, J.M., Brech, A., Callaghan, J., Toh, B.H., Murphy, C., Zerial, M., and Stenmark, H. (1998) EEA1 links PI(3)K function to Rab5 regulation of endosome fusion. *Nature* **394**, 494–498
47. Kyte, J. and Doolittle, R.F. (1982) A simple method for displaying the hydropathic character of a protein. *J. Mol. Biol.* **157**, 105–132
48. Lee, B. and Richards, F.M. (1971) The interpretation of protein structures: estimation of static accessibility. *J. Mol. Biol.* **55**, 379–400
49. Le Borgne, R., Alconada, A., Bauer, U., and Hoflack, B. (1998) The mammalian AP-3 adaptor complex mediates the intracellular transport of lysosomal membrane glycoproteins. *J. Biol. Chem.* **273**, 29451–29461
50. Dell'Angelica, E.C., Shorelersuk, V., Aguilar, W.A., Gahl, W.A., and Bonifacino, J.S. (1999) Altered trafficking of lysosomal proteins in Hermansky-Pudlack syndrome due to maturations in the β3A-subunit of the AP-3 adaptor. *Mol. Cell* **3**, 11–21
51. Peden, A.A., Oorschot, V., Hesser, B.A., Austin, C.D., Scheller, R.H., and Klumperman, J. (2004) Localization of the AP-3 adaptor complex defines a novel endosomal exit site for lysosomal membrane proteins. *J. Cell Biol.* **164**, 1065–1076
52. Jahraus, A., Storrie, B., Griffiths, G., and Desjardins, M. (1994) Evidence for retorograde traffic between terminal lysosomes and the prelysosomal/late endosome compartment. *J. Cell Sci.* **107**, 145–157
53. Futter, C.E., Pearse, A., Hewlett, L.J., and Hopkins, C.R. (1996) Multivesicular endosomes containing internalized EGF-EGF receptor complexes mature and then fuse directly with lysosomes. *J. Cell Biol.* **132**, 1011–1023
54. Bright, N.A., Gratian, M.J., and Luzio, J.P. (2005) Endocytic delivery to lysosomes mediated by concurrent fusion and kissing events in living cells. *Curr. Biol.* **15**, 360–365
55. Bright, N.A., Reaves, B.J., Mullock, B.M., and Luzio, J.P. (1997) Dense core lysosomes can fuse with late endosomes and are re-formed from the resultant hybrid organelles. *J. Cell Sci.* **110**, 2027–2040
56. Traub, L.M., Bannykh, S.I., Rodel, J.E., Aridor, M., Balch, W.E., and Kornfeld, S. (1996) AP-2-containing clathrin coats assemble on mature lysosomes. *J. Cell Biol.* **135**, 1801–1814